Proton Equilibria in the Manganese Cluster of Photosystem II Control the Intensities of the S_0 and S_2 State $g \approx 2$ Electron Paramagnetic Resonance Signals[†]

Paulina Geijer, Zsuzsanna Deák,[‡] and Stenbjörn Styring*

Biochemistry, Center for Chemistry and Chemical Engineering, Lund University, P.O. Box 124, S-221 00 Lund, Sweden

Received December 15, 1999; Revised Manuscript Received March 14, 2000

ABSTRACT: We have studied the pH effect on the S_0 and S_2 multiline electron paramagnetic resonance (EPR) signals from the water-oxidizing complex of photosystem II. Around pH 6, the maximum signal intensities were detected. On both the acidic and alkaline sides of pH 6, the intensities of the EPR signals decreased. Two p*K*s were determined for the S_0 multiline signal; $pK_1 = 4.2 \pm 0.2$ and $pK_2 = 8.0 \pm 0.1$, and for the S_2 multiline signal the p*K*s were $pK_1 = 4.5 \pm 0.1$ and $pK_2 = 7.6 \pm 0.1$. The intensity of the S_0-state EPR signal was partly restored when the pH was changed from acidic or alkaline pH back to pH $\approx$ 6. In the S_2 state we observed partial recovery of the multiline signal when going from alkaline pH back to pH $\approx$ 6, whereas no significant recovery of the S_2 multiline signal was observed when the pH was changed from acidic pH back to pH $\approx$ 6. Several possible explanations for the intensity changes as a function of pH are discussed. Some are ruled out, such as disintegration of the Mn cluster or decay of the S states and formal Cl^- and Ca^{2+} depletion. The altered EPR signal intensities probably reflect the protonation/deprotonation of ligands to the Mn cluster or the oxo bridges between the Mn ions. Also, the possibility of decreased multiline signal intensities at alkaline pH as an effect of changed redox potential of Y_Z is put forward.

Photosystem II (PSII)[1] is located in the thylakoid membrane of higher plants and algae. Upon illumination, plastoquinone is reduced on the acceptor side and water is oxidized to dioxygen on the donor side of PSII. The complex is composed of at least 25 different polypeptides (*1*). Two of these, the homologous polypeptides D1 and D2, form a heterodimer that binds the cofactors necessary for the electron transport: the primary electron donor, P680; the primary and secondary electron acceptor, pheophytin and quinone A (Q_A); the soluble two-electron carrier, quinone B (Q_B); and the two secondary electron donors, Y_Z (D1-Y161) and Y_D (D2-Y161). Of the two tyrosine residues, only Y_Z is involved in linear electron transport, while Y_D is an accessory electron donor (*2*, *3*).

Upon excitation, P680 donates an electron to pheophytin. To stabilize this charge-separated state, the electron is transferred to the acceptor Q_A and finally to Q_B. Rereduction of P680 occurs in nanoseconds by abstracting an electron from Y_Z. The resulting neutral Y_Z^{ox} radical is in turn reduced by the water-oxidizing complex (WOC) in 30−1300 μs depending on the oxidation state of WOC (*2*−*4*).

The water-oxidizing complex, interacting very closely with Y_Z (*5*−*8*), is composed of four Mn ions and the Ca^{2+} and Cl^- cofactors. The D1/D2 heterodimer contain most of the putative amino acid ligands to the Mn cluster (see ref 9 for a review). The structure of the Mn cluster is not yet determined. From different spectroscopic measurements the most favored structure is two di-μ-oxo bridged Mn dimers connected with two carboxylato bridges and one mono-μ-oxo bridge (*3*, *4*, *10*, *11*). Several other models have also been proposed to explain the available data (*12*−*14*). The Ca^{2+} and Cl^- ions are important for the function of the Mn cluster but their exact positions in the WOC are unknown (*3*, *4*, *10*). The Mn cluster binds two water molecules that are the ultimate electron donors to PSII. During water oxidation the Mn cluster cycles through five different oxidation states, denoted S_0−S_4, where the index represents the number of stored oxidizing equivalents (*15*). The S_1 state is the dark-stable state. The S_2 and S_3 states are intermediate states with high midpoint redox potentials and decay to the S_1 state on a seconds time scale. The S_4 state is an intermediate state where the $S_3 \rightarrow S_4$ is a light-induced transition and dioxygen is evolved during the spontaneous $S_4 \rightarrow S_0$ transition. The least oxidizing S_0 state decays to the S_1 state in tens of minutes (*3*, *4*, *10*, *16*, *17*).

Electron paramagnetic resonance (EPR) spectroscopy is a useful tool for studying the different S states of the Mn cluster. Figure 1 shows the Mn EPR signals centered around $g = 2$ from the S_0 and S_2 states studied in this work. The multiline EPR signal from the S_2 state was reported in 1981

[†] Financial support from the Sven and Lily Lawski Foundation (P.G.), the Knut and Alice Wallenberg Foundation, the Crafoord Foundation, the Swedish Natural Science Research Council (Z.D.), and the European TMR program (TMR CT96-0031) is gratefully acknowledged.

* Corresponding author: phone +46 46 222 01 08; fax +46 46 222 45 34; e-mail stenbjorn.styring@biokem.lu.se.

[‡] Permanent address: Institute of Plant Biology, Biological Research Center, Hungarian Academy of Science, P.O. Box 521, H-6701 Szeged, Hungary.

[1] Abbreviations: Chl, chlorophyll; DMSO, dimethyl sulfoxide; EDTA, ethylenediaminetetraacetic acid; EPR, electron paramagnetic resonance; Hepes, 4-(2-hydroxyethyl)piperazineethanesulfonic acid; Mes, 4-morpholinoethanesulfonic acid, PpBQ, phenyl-*p*-benzoquinone; PSII, photosystem II; SII_{slow}, the electron paramagnetic resonance signal from the neutral Y_D^{ox} radical; WOC, water-oxidizing complex; Y_Z and Y_D, the two redox-active tyrosine residues D1-161 and D2-161 in PSII.

10.1021/bi992878c CCC: $19.00
Published on Web 05/12/2000

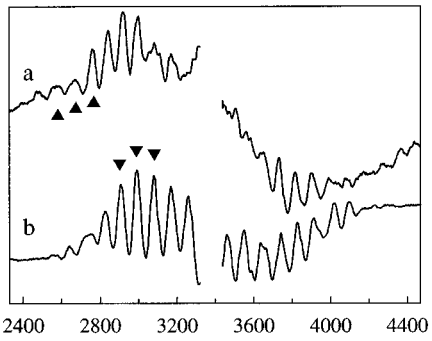

FIGURE 1: S_0 and S_2 multiline EPR signals recorded after (a) 3 flashes and (b) 1 flash. The peaks used for evaluation of the S_0 and S_2 signal amplitudes throughout this study are indicated with triangles. The SII_{slow} region has been omitted for clarity. The S_2 multiline has been scaled to $^1/_4$ of its actual size. EPR settings: microwave power 56 mW (S_0) and 12 mW (S_2); microwave frequency 9.47 GHz; temperature 7 K; modulation frequency 100 kHz; modulation amplitude 20 G.

(*18*). The S_2 multiline signal is approximately 1900 G wide and was proposed to arise from an antiferromagnetically coupled Mn cluster with total spin $S = {}^1/_2$, where two Mn ions possess the Mn(III) and Mn(IV) oxidation states (*10*, *18*, *19*). The S_0 state, being two electrons more reduced than the S_2 state, was long expected to be paramagnetic but it was not until 1997 shown to have an EPR signal (*20*, *21*). The S_0-state multiline signal is wider (2500−2800 G) than the S_2 multiline signal and also arises from a $S = {}^1/_2$ Mn cluster, now with the Mn(II) and Mn(III) oxidation states present (*20*−*22*).

Many of the catalytic events on the donor side in PSII display pH dependencies (*17*, *23*−*29*). Extreme pHs are known to inhibit O_2 evolution, and studies also show that oxidation and reduction of both Y_Z and Y_D are pH-dependent. Since the rereduction of Y_Z is very fast in the presence of the Mn cluster, most studies have been performed in Mn-less systems where the rates are slowed. These studies show that the electron-transfer rate between Y_Z and P680 has an apparent p*K* of 7−8, dependent on the material used (*28*−*30*). Direct influence of pH on the Mn cluster has also been studied (*31*−*33*). In these studies the effect of pH on the S-state transitions have been probed with thermoluminescence measurements and EPR spectroscopy on the S_2 multiline signal. Vass et al. (*31*) showed with thermoluminescence that a mild alkaline treatment of thylakoids led to the inhibition of the $S_3 \rightarrow S_4$ transition. Ono and Inoue (*32*) showed that the S_2 multiline EPR signal arising after the $S_1 \rightarrow S_2$ transition in acidic conditions was very similar to the S_2 multiline observed in Ca^{2+}-depleted samples. It has also been shown that if PSII-enriched membranes in the S_1 state are incubated at alkaline pH in darkness, most of the centers stay intact (*33*). In conclusion, it is known that the Mn cluster in the S_1 state is only slightly sensitive to damage by alkaline pH whereas the S-state transitions are very sensitive to extreme pHs.

Until now the direct influence of pH on the EPR signals from the S_0 and S_2 states has never been studied. There now exist useful spectroscopic probes from the S_0 and S_2 states that make it possible to directly study the Mn cluster when subjected to changes in pH. In this study EPR spectroscopy has been used to investigate the direct effects of pH on the S_0 and S_2 multiline signals. The pH has been changed in the respective S state *after* the exciting flashes and the results show that the amplitude of the S_0 and S_2 multiline EPR signals are drastically, and partly reversibly, decreased.

Scheme 1

Titration:

$$\text{Flash(es)} \longrightarrow \Delta\text{pH} \xrightarrow{\text{Freeze}} \text{EPR}$$

Reversibility:

$$\text{Flash(es)} \xrightarrow{\text{Freeze}} \text{EPR} \xrightarrow{\text{Thaw}} \Delta\text{pH} \xrightarrow{\text{Freeze}} \text{EPR} \xrightarrow{\text{Thaw}} -\Delta\text{pH} \xrightarrow{\text{Freeze}} \text{EPR}$$

MATERIALS AND METHODS

PSII Membrane Preparation. PSII-enriched membranes were prepared according to ref *34* from spinach grown on liquid culture medium. The preparations were stored at −80 °C at approximately 10 mg of Chl/mL. All chlorophyll determinations were made in 80% ice-cold acetone according to ref *35*. The oxygen evolution was 350−400 μmol of O_2 (mg of Chl)$^{-1}$ h^{-1}.

pH Titration. PSII-enriched membranes were diluted approximately 5 times with a low-buffering medium, A (0.5 mM Mes/KOH, 400 mM sucrose, 10 mM NaCl, 10 mM $MgCl_2$, and 5 mM $CaCl_2$, pH 6.0), with 5 mM EDTA, centrifuged for 15 min at 40 000*g*, and resuspended in medium A, this time without EDTA. The EPR samples were then prepared in calibrated EPR tubes with final concentrations of ∼4 mg of Chl/mL and 5% (v/v) methanol. Before the flash protocol, the samples were given 3 min of room light, to fully oxidize Y_D, followed by a 10 min dark adaptation. This results in a mixture of $S_0Y_D^{ox}$ (25%) and $S_1Y_D^{ox}$ (75%) centers. To synchronize 100% of the PSII centers in the $S_1Y_D^{ox}$ state, the samples were treated with a preflash protocol as in ref *16* with an 18 min dark incubation (20 °C) between the preflash and the exciting flashes (one flash to obtain the S_2 state and three flashes to obtain S_0). The external acceptor, P*p*BQ (dissolved in DMSO), was added 1 min before the exciting flashes to a final concentration of 0.5 mM. After 1 flash, 75−80% of the PSII centers were in the S_2 state, and the rest were in the S_1 state. Three flashes result in about 50−60% S_0-state population with the remaining centers in the S_2 and S_3 states. The amount of each S-state is determined from oscillations from the multiline EPR signals as described in refs *16* and *20*. The flashes (6 ns, 532 nm, 350 mJ) were given at 5 Hz from a Nd−YAG laser (Spectra Physics). The pH was adjusted immediately *after* the exciting flashes (Scheme 1), by adding buffer solutions in the pH range 4.0−9.0: DL-glutamic acid/KOH (pH 4.0−5.0), Mes/KOH (pH 5.0−7.0), Hepes/KOH (pH 7.0−8.0), or glycylglycine/KOH (pH 8.0−9.0). The final buffer concentration was 14 mM. The samples were frozen 30 s after the flashes. To allow thorough mixing, the buffers were added with a syringe with a spiral shaped tip. All steps were performed in dim green light. After the EPR measurements the samples were thawed and the final pH, steady-state O_2 evolution, and Chl concentration were determined. The pH was determined with a small-tip standard pH electrode after transfer of the EPR samples to Eppendorf tubes.

pH Reversibility. To study the reversibility of the pH effects, samples were prepared in the same way as described above except that immediately after the exciting flashes the samples were frozen for EPR measurements (Scheme 1). After this EPR measurement, the samples were thawed and the first pH change was made (addition 1, 14 mM final concentration of the pH buffer). The samples were again frozen and the EPR measurements repeated. The samples were thawed again and the pH was changed back to pH ≈ 6 (addition 2, 40 mM Mes final concentration) and frozen again for the final EPR measurements (Scheme 1). After each pH addition (addition 1 and 2) the samples were incubated for 30 s to allow mixing before freezing. Parallel samples with only addition 1 were made to determine the obtained pH. During the thawing procedures the time was carefully monitored to allow estimation of the decay of the S_0- and S_2-state populations that occur during the experiments. The S_0 state decays with different half-times in a pH-dependent manner in an oxidation reaction with Y_D^{ox} (*16*, *17*). The half-times used for the estimation of the decay of the S_0 signal at pH 4.4, 5.8, and 8.5 of 45, 15, and 8 min, respectively. These values were taken from the study by Vass and Styring (*17*), where they studied the pH-dependent decay of the Y_D^{ox} EPR signal via the $S_0Y_D^{ox} \rightarrow S_1Y_D$ reaction. The S_2 state can decay via a reaction with Y_D: $S_2Y_D \rightarrow S_1Y_D^{ox}$. This reaction is pH-dependent (*17*, *36*) but does not occur in our samples since Y_D was fully oxidized. Instead the dominating decay of the S_2 state is a slower reaction, with electrons from other sources, which also is pH-dependent. The half-times of the S_2 state decay at pH 4.5, 6, and 8.5 are 100, 340, and 240 s, respectively, and were determined in intact thylakoids by Messinger and Renger (*36*). Our samples were incubated at 15−20 °C during the additions of buffers whereas the half-times for the S_2-state decay were determined at 10 °C (*36*). This would mean that our half-times for the S_2-state decay are faster and that we probably underestimate the amount of S_2 multiline signal in our samples when we normalize to the decay of the S_2 state.

EPR and Data Analysis. Low-temperature continuous-wave EPR measurements were performed with a Bruker ESP380e spectrometer fitted with a liquid helium cryostat and temperature controller (Oxford Instruments Ltd.). Spectrometer settings are given in the figure legends. The intensities of the S_0 and S_2 multiline EPR signals were estimated by the sum of the amplitudes of three peaks, indicated with triangles in Figure 1. The intensities were normalized to the size of SII_{slow} to compensate for differences in sample concentration and tube diameter.

The titration curves from both the S_0 and S_2 signals are fitted from pH 4.5 to 8.5 with a combination of two p*K*s. We assume that the EPR signal amplitude (y) is proportional to the concentration of EPR-visible WOC ([AH]) according to eq 1 (the doubly protonated $[AH_2^+]$ and deprotonated $[A^-]$ states are assumed to be EPR invisible):

$$y = k[\mathrm{AH}] \quad (1)$$

The total concentration of WOC (A_t) is the sum of the EPR-visible and -invisible forms according to

$$A_t = [\mathrm{AH_2}^+] + [\mathrm{AH}] + [\mathrm{A}^-] \quad (2)$$

The Henderson−Hasselbalch relations of $[AH_2^+]$ and $[A^-]$ are given in

$$[\mathrm{AH_2}^+] = [\mathrm{AH}]/10^{\mathrm{pH}-\mathrm{p}K_1} \quad (3)$$

$$[\mathrm{A}^-] = [\mathrm{AH}]10^{\mathrm{pH}-\mathrm{p}K_2} \quad (4)$$

By inserting eqs 3 and 4 into eq 2, and solving it for [AH], and then inserting the resulting equation into eq 1, we obtain

$$y = c/(1 + 10^{\mathrm{p}K_1-\mathrm{pH}} + 10^{\mathrm{pH}-\mathrm{p}K_2}) \quad (5)$$

where y is the measured EPR signal amplitude, pK_1 is the apparent p*K* at low pH, and pK_2 is the apparent p*K* at high pH and the proportionality constant $c = kA_t$.

Steady-State O_2 Evolution. Steady-state O_2 evolution was measured with a Clark-type electrode at 20 °C in a medium containing 20 mM Mes/KOH, 10 mM $MgCl_2$, 10 mM NaCl, 5 mM $CaCl_2$, and 400 mM sucrose at pH 6.0, with PpBQ (in DMSO, 0.5 mM final concentration) added as the external acceptor. Illumination was supplied from a saturating white-light source. Directly after the EPR samples were thawed, 20 μg Chl of each EPR sample was added to 1 mL of medium. The O_2 evolution was always measured at pH 6, irrespective of the pH of the sample.

RESULTS

pH Titration of the S_0-State Multiline Signal. In our experiment, we have formed the S_0 state by three powerful laser flashes given at pH 6.0. Immediately after the flashes, the pH was altered and the EPR spectrum was recorded (Scheme 1). Thus, we study the pH effects on the S_0 state itself and not on the S-state transitions to S_0. The S_0 multiline EPR signal at four different pH values (4.4, 5.8, 7.5, and 8.5) is shown in Figure 2A. The largest signal amplitude is measured around pH 5.8 (set to 100% in Figure 2B). When the pH was either decreased to 4.4 or increased to 8.5, the signal amplitude decreased successively. The hyperfine structure seems unaffected by pH; only the amplitude of the hyperfine peaks changes.

A pH titration of the S_0 EPR signal amplitude was performed from pH 4.4 to 8.5, with an interval of approximately 0.25 pH unit between each sample. The titration curve in Figure 2B shows that the amplitude of the S_0 multiline signal is altered by pH. The S_0 multiline signal has maximum amplitude around pH 6 and the amplitude decreases on both sides of this region. The signal intensity at pH 4.4 is 40% of the maximum, and at pH 8.5, 20% of the maximum S_0 signal is detected. The change of the S_0 EPR signal intensity with pH in Figure 2B has been fitted from pH 4.4 to 8.5 with eq 5, where we take into account different events appearing at acidic (pK_1) and alkaline (pK_2) pH, respectively. These two events give rise to the complex titration curve observed in Figure 2B. The fitting resulted in two apparent p*K*s of 4.2 ± 0.2 and 8.0 ± 0.1. However, visual inspection of the fit and the data suggests that the titration might be more complex, potentially involving more than two p*K*s. A preliminary study of this effect of pH on the S_0 multiline based on a limited data set has been reported, providing an approximate alkaline p*K* of 7.6−8.1 (*37*). Here we present a more detailed study and the pK = 8.0 is well in line with our previous approximation.

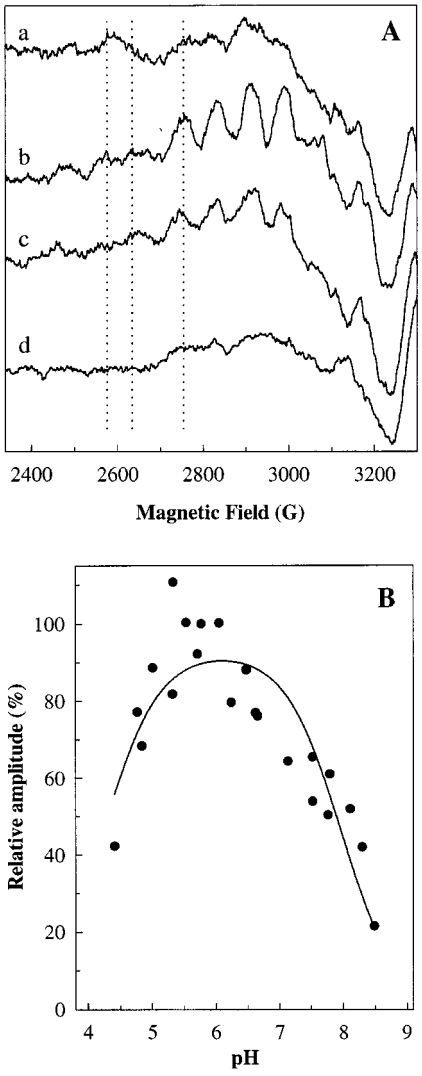

FIGURE 2: (A) S_0 state EPR signal at four different pH values: (a) pH 4.4, (b) pH 5.8, (c) pH 7.5, and (d) pH 8.5. The dotted lines indicate the positions of the three peaks used for the determination of the spectral intensities in the titration curve in panel B. The spectra are normalized to the double integral of SII_{slow}. Contributions from the S_2 multiline signal have been subtracted, based on different microwave power settings and the EPR signal oscillation patterns, so that the S_2 multiline contributions close to the radical region are minimized (*20*). EPR settings: microwave power 58 mW; microwave frequency 9.47 GHz; temperature 7 K; modulation frequency 100 kHz; modulation amplitude 20 G. (B) pH titration curve from pH 4.4 to 8.5 of the S_0 EPR signal amplitude as percent of the spectral intensity of the pH 5.8 sample. The data points reflect the sum of three peak amplitudes (indicated with dotted lines in panel A) of the S_0 state EPR signal recorded after three flashes and subsequent pH change. The fitting of the curve from pH 4.5 to 8.5 was made with eq 5 as described under Materials and Methods and yielded apparent p*K*s of 4.2 ± 0.2 and 8.0 ± 0.1 of the decrease of the S_0 state signal.

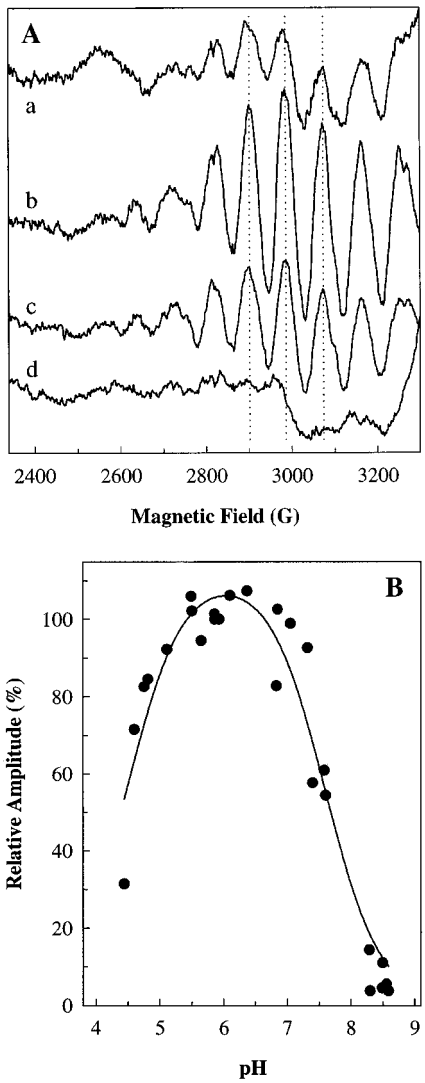

FIGURE 3: (A) S_2 state EPR signal recorded after 1 flash and subsequent pH change at four different pH values: (a) pH 4.4, (b) pH 5.9, (c) pH 7.6, and (d) pH 8.6. The dotted lines indicate the peaks used for the estimation of the signal amplitude. EPR settings: microwave power 13 mW; microwave frequency 9.47 GHz; temperature 7 K; modulation frequency 100 kHz; modulation amplitude 20 G. (B) pH titration curve of the spectral change of the S_2 multiline signal from pH 4.4 to 8.6 as percent of the amplitude in the pH 5.9 sample. The data points are obtained as in Figure 2. The fitting of the curve (described under Materials and Methods) gave apparent p*K*s of 4.5 ± 0.1 and 7.6 ± 0.1 for the decrease of the S_2 multiline signal.

pH Titration of the S_2-State Multiline Signal. The pH dependence of the S_2 multiline signal in samples given one flash was also investigated. In Figure 3A, the S_2 multiline at four different pH values (4.4, 5.9, 7.6, and 8.6) is shown. The intensity of the S_2 multiline also shows a strong pH dependence. The S_2 multiline has the maximum amplitude between pH 5.5 and 6.5, whereas at pH 4.4 30% of the signal is detected and at pH 8.6 only 5% of S_2 multiline amplitude remains (Figure 3B). The apparent p*K*s of the loss of the S_2 multiline signal were estimated with eq 5 as $pK_1 = 4.5 \pm 0.1$ and $pK_2 = 7.6 \pm 0.1$. This is similar to the apparent p*K*s obtained for the S_0 multiline. The data were fitted nicely with two p*K*s (Figure 3B).

The experiments presented so far were performed in the presence of 5% (v/v) methanol, which allows the detection of the S_0 multiline signal (*38*, *39*) and the maximum amplitude of the S_2 multiline signal. An experiment to investigate if methanol in some way interferes with the decrease of the S_2 multiline signal was made. A similar decrease of the S_2 multiline signal amplitude was detected in samples at pH 8.6 both with and without methanol (data not shown), indicating that methanol does not interfere with the titration of the S_2 multiline signal.

pH Dependence of SII_{slow} and O_2 Evolution and Integrity of the Mn Cluster. In every sample, SII_{slow} was monitored

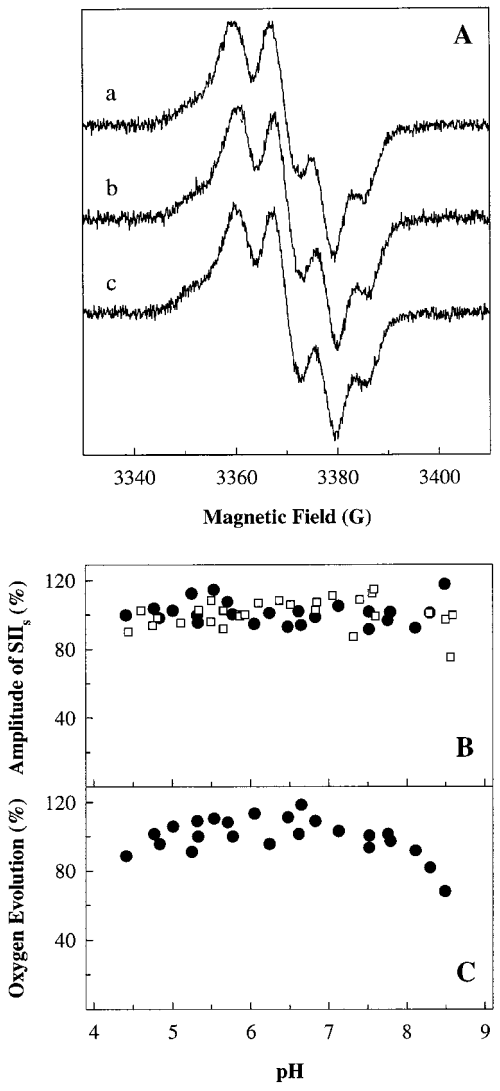

FIGURE 4: (A) Tyr_Dox EPR signal is unaffected by pH. Signal II_{slow} was recorded at three different pH values: (a) 4.4, (b) 5.8, and (c) 8.3 in samples from Figure 2. The signals are normalized for differences in chlorophyll concentration. EPR settings: microwave power 1.16 μW; microwave frequency 9.47 GHz; temperature 15 K; modulation frequency 100 kHz; modulation amplitude 3.2 G. (B) Double integral of signal II_{slow} from the samples in Figure 2 (•) and 3 (□) as a function of pH. The signals are normalized to the size of signal II_{slow} at pH 5.8 (•) and 5.9 (□), respectively. (C) Oxygen evolution in the samples from Figure 2. After the EPR measurements, the samples were thawed and aliquots were added to a Clark-type electrode with a medium at pH 6 where the oxygen evolution was measured. The oxygen evolution rates are normalized to the rate at pH 5.8. The O_2 evolution in the pH 5.8 sample was 80% of the steady-state O_2 evolution in freshly prepared PSII-enriched membranes.

to see whether Y_D^{ox} became reduced during the incubation, thus causing the decrease of the S_0 multiline signal. Also, the pH might alter the redox equilibria on the donor side of PSII, resulting in the formation of Y_Z^{ox} or some other oxidized radical component in addition to Y_D^{ox} (see Discussion). As shown in Figure 4, the amplitude of SII_{slow} was largely unaffected by pH in both the one- and three-flash experiments.

The integrity of the Mn cluster can be studied with EPR by observation of free Mn^{2+}. If the EPR signal from free Mn^{2+} is detected, some of the Mn clusters have become damaged and started to disintegrate. The pH change and the 30 s incubation between flashes and freezing of the samples used for the titration experiment in Figures 2 and 3 causes no detectable manganese release (data not shown). This indicates that the Mn cluster remained intact during the experiment. Consequently, the S_0 and S_2 multiline EPR signals were not lost due to Mn^{2+} release from the Mn cluster.

Measurements of the ability to carry out steady-state oxygen evolution after the pH treatment confirm the presence of an intact Mn cluster. The pH optimum for the steady-state O_2 evolution is between 5.5 and 6.5 (*17*). At pH values outside this range, the O_2 evolution decreases drastically, and measurements provide little information about the intactness of the Mn cluster. Therefore, the steady-state O_2 evolution was measured around pH 6.0 after the EPR measurements when the samples were thawed. An aliquot from each EPR sample was transferred to the oxygen electrode at pH 6 and the activity was measured. The rates were largely unaffected by the pH treatment. More than 70% of the maximum oxygen evolution was detected in all samples from the pH titration series, including the high-pH samples, where as much as 80% and 95% of the S_0 and S_2 multilines, respectively, had been lost (Figure 4C). The $\approx$30% loss of the O_2 evolution at extreme pHs could be explained by the release of some Mn^{2+} during the thawing of the EPR samples for O_2-evolution measurements.

Thus, we can conclude that the S_0 and S_2 multiline signals were not lost due to damage and loss of the Mn cluster by the pH treatment. Also, the loss of the S_0 multiline signal with pH was not caused by the interaction with Y_D^{ox}. Instead, the multiline signals are decreased due to other, more complex, reasons.

Reversibility of the Loss of the S_0 and S_2 Multiline Signals. Our control experiments presented above show that the Mn cluster remains intact after the pH treatment. This indicates that the loss of the S_0 and S_2 multiline signals at alkaline and acidic pH could be due to loss of the S_0 and S_2 states, respectively. Another possibility for the loss of the multiline signals is that the pH treatment reflects reversible protonation/deprotonation events in the vicinity of the Mn cluster. To test these alternatives, reversibility experiments were performed where the pH was changed back from extreme pH to normal pH (pH 6).

In Scheme 1, the outline of the reversibility experiment is shown. Preflashed samples at pH 6 were given the exciting flashes. The samples were immediately frozen for EPR measurements. The first change of pH (either acidic or alkaline) was made and the EPR measurements were repeated. To change back the pH to 6, a second pH addition was made and the final EPR measurements were performed. In Figure 5A the EPR spectrum of a S_0 sample where the pH was altered to pH 8.6 and then back to pH 6.2 is shown. The maximum intensity is observed when the sample was frozen directly after the flashes (Figure 5A, spectrum a). After the first change of pH (to pH 8.6), 25% of the maximum intensity was detected (Figure 5A, spectrum b). When this sample was thawed and the pH was readjusted to 6.2, the S_0 multiline signal reappeared and 38% of the maximum signal intensity was observed (Figure 5A, spectrum c). This clearly shows that the loss of the S_0 multiline at high pH was reversible.

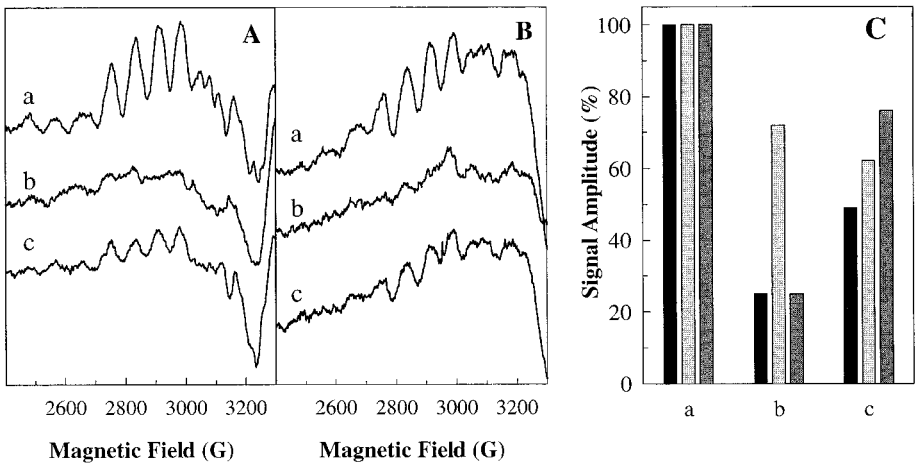

FIGURE 5: Reversibility of the pH-induced decrease of the S_0 multiline signal intensity. (A) Reversibility at alkaline pH. The three spectra represent the S_0 multiline (a) after 3 flashes at pH 5.8, (b) after the sample has been thawed and the pH changed to 8.6, and (c) after a second change of pH back to 6.2. (B) Reversibility at acidic pH. The three spectra represent the S_0 multiline (a) after 3 flashes at pH 6.0, (b) after the sample has been thawed and the pH changed to 4.5, and (c) after a second change of pH to 6.1. The EPR spectra in panels A and B are normalized to the dilution of the sample to account for changes in concentration during the additions. The spectra have not been corrected for any decay of the S_0 state. Contributions from remaining S_2 multiline signal were subtracted as in Figure 2. (C) Bar diagram illustrating the reversibility of the pH-dependent decrease of the S_0 state multiline signal. The amplitudes have been normalized to the decay of the S_0 state at different pHs as described under Materials and Methods. Black bars show amplitude of the S_0 signal (a) directly after flashing (pH 6.0), (b) after changing the pH to 4.5, and (c) after changing the pH back to pH 6.1. Light gray bars show amplitude at pH 6.0 after the same dilution and mixing but without changing the pH. Dark gray bars show amplitude of the S_0 signal (a) directly after flashing (pH 5.8), (b) after changing the pH to 8.6, and (c) after changing the pH back to pH 6.2. The amplitudes of the S_0 multiline signal are determined as in Figure 2A.

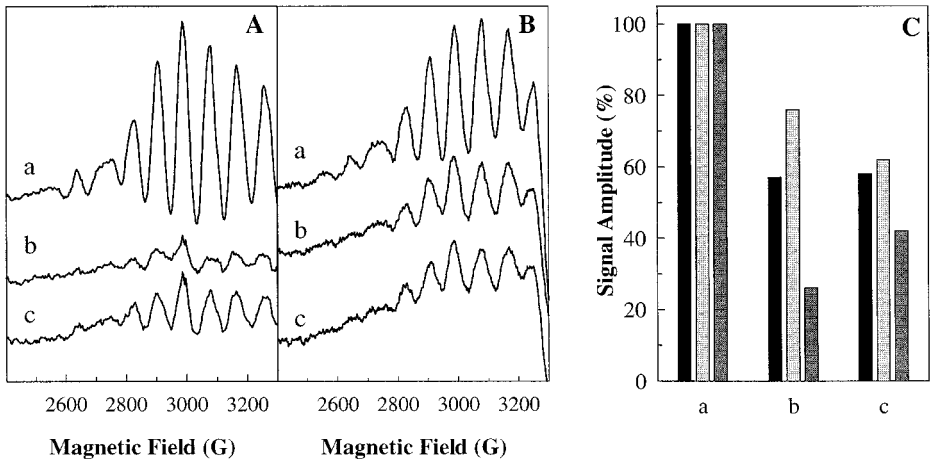

FIGURE 6: Reversibility of the pH-induced decrease of the S_2 multiline signal intensity. (A) The three spectra represent the S_2 multiline (a) after 1 flash at pH 6.1, (b) after the sample has been thawed and the pH changed to 8.5, and (c) after a second change of pH to 6.4. (B) The three spectra represent the S_2 multiline (a) after 1 flash at pH 6.1, (b) after the sample has been thawed and the pH changed to 4.5, and (c) after a second change of pH to 6.0. The EPR spectra in panels A and B are normalized to the dilution of the sample to account for changes in concentration during the additions. The spectra have not been corrected for any decay of the S_2 state. (C) Bar diagram illustrating the reversibility of the pH-dependent decrease of the S_2-state multiline signal. The amplitudes have been normalized to the decay of the S_2 state at different pHs as described under Materials and Methods. Black bars show amplitude of the S_2 signal (a) directly after flashing (pH 6.0), (b) after changing the pH to 4.5, and (c) after changing the pH back to pH 6.1. Light gray bars show amplitude at pH 6.0 after the same dilution and mixing but without changing the pH. Dark gray bars show amplitude of the S_2 signal (a) directly after flashing (pH 6.1), (b) after changing the pH to 8.5, and (c) after changing the pH back to pH 6.4. The amplitudes of the S_2 multiline signal are determined as in Figure 3A.

The reversibility of the S_0 multiline at acidic pH is shown in Figure 5B. The EPR spectra a−c represent the maximum signal, the signal after pH change to 4.5, and the signal after pH change to pH 6.1, respectively. At pH 4.5, 27% of the signal intensity was observed, and when the pH was readjusted to 6.1, 45% of the signal amplitude was detected (Figure 5B, spectra b and c). In Figure 5C the changes of the S_0 multiline intensities at the different pH changes are presented, corrected for the known decay of the S_0 state (see Materials and Methods). The black bars represent the reversibility at acidic pH, the light gray bars illustrate a control experiment where only buffer with pH 6 was added, and the dark gray bars show the reversibility at alkaline pH.

The reversibility of the S_2 multiline was probed in the same way as for the S_0 multiline signal. Figure 6A shows three EPR spectra of the S_2 multiline; without any addition (a), at pH 8.5 (b), and at pH 6.4 when the pH of the sample was changed back (c). At pH 8.5 only 12% of the maximum amplitude of the S_2 multiline is observed (Figure 6A, spectrum b). This amplitude increases to 25% when the pH

is changed back to pH 6.4 (Figure 6A, spectrum c). In Figure 6B the same experiment on the S_2 multiline at acidic pH is presented. The change of pH to 4.4 resulted in detection of 41% of the maximum amplitude (Figure 6B, spectrum b), whereas 36% of the signal was detected when the sample was changed back to pH 6.0 (Figure 6B, spectrum c). In Figure 6C the changes of the signal intensities after the different pH changes are normalized to the decay of the S_2 state. Here we see that the decreased intensity at acidic pH is not recovered, whereas at alkaline pH there is recovery of the signal intensity (Figure 6C). The half-times used for the estimation of the S_2-state decay were determined at 10 °C (*36*). We make our pH additions at 15−20 °C. Thus, we underestimate the amount of S_2 state in our samples after the incubations when we have normalized to the expected decay of the S_2 state.

The reversibility experiments clearly show that the loss of the S_0 and S_2 multilines at alkaline pH are reversible, whereas at acidic pH the reversibility is less pronounced, especially for the S_2 multiline signal. We conclude that the decreased intensities of the S_0 and S_2 multiline signals at alkaline pH probably is not due to a loss of the formal redox states of S_0 and S_2. Instead the results indicate that there is some protonation/deprotonation event occurring in the Mn cluster or in the vicinity of the cluster. It is likely that a similar explanation is valid for the reversible part of the reaction at acidic pH.

DISCUSSION

The data presented in this work show that the S_0 and S_2 multiline EPR signals are affected by the pH of the solution. At pHs known to inhibit the steady-state O_2 evolution (below ≈5.5 and above ≈7.2) we see that the Mn EPR signals are lost reversibly. The obtained p*K*s for the titrations in the S_0 (4.2 and 8.0) and S_2 states (4.5 and 7.6) are similar to each other. This similarity have important implications for the view of charge neutrality in WOC. If there was a buildup of charge in WOC during the turnover of the S states, this would affect the p*K*s of the S_0 and S_2 states (Gerald Babcock, personal communication). It should be noted that the pH-induced changes of the Mn EPR signals in both S_0 and S_2 is the second type of modification that has effects on both S_0 and S_2. The other reagent reported so far to have effects in both S states is methanol, which makes the S_0 multiline signal observable and shifts the $g = 4.1$ signal to the multiline form in the S_2 state (*20*, *21*, *38*, *39*).

What are the changes in PSII that cause the loss of the S_0 and S_2 multiline EPR signals at acidic and alkaline pH? We see several possibilities: (i) It could be a loss or damage of the Mn cluster during the pH treatment; (ii) the S_0 and S_2 states could irreversibly decay to S_1 or another diamagnetic redox state; (iii) a structural change of the Mn cluster or its ligands in either S state could alter the magnetic couplings; (iv) the pH could alter the redox equilibrium involving the Mn cluster and Y_Z; or (v) there could be a combination of these effects.

From the results presented above we can immediately exclude possibilities i and ii. The Mn cluster remains intact during the pH treatment. There is no release of free Mn^{2+} detected during the EPR measurements, and more importantly, the steady-state O_2 evolution (at pH = 6.0) was virtually unchanged by the pH treatment. Also, the irreversible decay of the S states during the pH treatment (possibility ii) is excluded by the reversibility experiments. In both S_0 and S_2 the EPR multiline signals were retrieved upon going back from alkaline pH to approximately pH 6. The differences between the actual recovery and the expected maximum recovery calculated from the known decay of S_0 and S_2 (Figures 5C and 6C for S_0 and S_2, respectively) can probably be accounted for by the precision in the data and some destruction of the cluster (≤30% as determined from the O_2 evolution) due to repeated thawing. Our reversibility studies at acidic pH are less conclusive. The less pronounced reversibility at acidic pH could indicate that different processes are involved in the decrease of the signal amplitudes at alkaline and acidic pH. One explanation for the poor reversibility at acidic pH is the appearance of an unknown donor to OEC, below pH 5. Experiments are in progress to identify a donor that can react with both the S_0 and S_2 states at acidic pH. However, as judged from the O_2-evolution measurements, the signals are not lost due to damage of the Mn cluster.

Thus, the reversibility experiments strongly suggest that the centers are in the formal S_0 and S_2 states when subjected to extreme pHs. The loss of EPR-observable signals from the Mn cluster in these S states must therefore involve some other change in the water-oxidizing complex. The modifications are likely to involve either (iii) structural changes in the Mn cluster itself or among its ligands or (iv) alterations of the redox equilibria in the WOC (including Y_Z and potentially other redox-active groups). Below we will discuss each of these possibilities in further detail.

Structural changes in the Mn cluster such as depletion of Ca^{2+} or Cl^- are known to modify the magnetic properties of the Mn cluster. Many studies have been made on how the depletion of chloride and calcium affect the activity of PSII (see refs *10* and *40*−*45* for a compilation). All the studies show that the turnover of the S cycle is inhibited or slowed at the S_3 state. The treatments to deplete calcium and chloride often include a pH treatment at extreme pHs (Cl^- depletion at alkaline pH and Ca^{2+} depletion at acidic pH) (reviewed in refs *40*, *41*, and *44*). One possibility for the disappearance of the multiline signals in our samples could be that the altered pH depletes the calcium and chloride ions. However, with the high concentrations of Ca^{2+} (4−5 mM) and Cl^- present (30−35 mM) in all the samples compared to the binding constants for Ca^{2+} and Cl^- (*44*), we rule this out.

We also investigated the alkaline pH-induced (pH 8.5) loss of the S_0 multiline in the presence of 100 mM Cl^- (data not shown). There was no change in the relative amplitude between the samples at pH 8.5 and pH 6 in 100 mM Cl^- compared to samples in 30−35 mM Cl^-. In this study we find it unlikely that there is a formal Ca^{2+} and Cl^- depletion. A possibility could still be that there is a local equilibrium that dislocates the Ca^{2+} and Cl^- ions but that they remain in the vicinity of the Mn cluster (*46*).

Other pH-induced structural and chemical changes that could alter the EPR signals from the S_0 and S_2 states could be direct titration of the oxo bridges in the Mn cluster. The protonation states of the oxo bridges in the different S states are not known. However, from comparison with model compound chemistry, models have been proposed, where the

protonation state of the oxo bridges vary with S state (ref *11* and references therein; Holger Dau, personal communication).

The decrease of the S_0 and S_2 multilines at acidic pH may be caused by the protonation of an oxo bridge in the Mn cluster. Protonation of oxo bridges in several Mn-compounds has been studied (*47*−*49*). Protonation of an oxo bridge in a Mn complex increases the distance between the Mn atoms, thereby decreasing the antiferromagnetic exchange coupling between the Mn ions (*48*). Exactly how this would apply to the magnetic couplings in the WOC and thereby the S_0 and S_2 EPR signals is not easy to predict. However, a pH-dependent equilibrium between one strongly and one weakly antiferromagnetically coupled Mn(III)Mn(III) state has been detected in Mn-catalase with magnetic susceptibility measurements (*50*). A weakly antiferromagnetically coupled state, with *J* approximately zero, would not give distinct hyperfine lines of the multiline signal and may not be EPR-detectable at all. Population of such a state could explain the decrease of the S_0 and S_2 EPR signals.

The decrease of the signals at alkaline pH may be explained in an analogous way. If the Mn cluster is protonated in vivo, deprotonation of an already protonated oxo bridge is expected to decrease the distance between the Mn ions involved. This is likely to increase the exchange coupling between the Mn ions, leading to altered EPR signals. Also in this situation it is difficult to foresee how the exchange couplings involving the other Mn ions would be affected.

A different category of pH-induced changes in and around the Mn cluster involves titration of substrate water (or derivatives) or amino acid residues interacting with the Mn ions. The ligands to the Mn cluster are not conclusively identified but the most likely candidates are glutamate, aspartate, and histidine residues (*51*−*58*). A protonation or deprotonation of one of these ligands or substrate water (derived) molecules could affect the magnetic properties of the Mn cluster such that the EPR signals from the S_0 and S_2 states would decrease in a similar manner. A titration of one or more of the carboxylato ligands could be the origin of the loss of the Mn signals at acidic pH, and a histidine residue could be involved at alkaline pH.

It is interesting to note that a histidine residue with a p$K_a \approx 7-7.5$ was proposed to control electron donation from Mn^{2+} to Mn-depleted PSII centers (*55*, *59*). Furthermore, His190 on the D1 protein, a residue that is thought to be hydrogen-bonded to Y_Z and close to the Mn cluster (*30*, *59*−*62*), is thought to have a p*K* between 7 and 8. A titration of a histidine ligand to the Mn cluster could occur close to the alkaline p*K* we observe, and this would interfere with the properties of the EPR signals at alkaline pH.

Amino acid residues that are modulated by the oxidation state of the Mn cluster were proposed by Rappaport and Lavergne (*63*) by pH-dependence studies on the proton release pattern during the S cycle. They observed that several amino acids with different p*K*s are involved in the proton release. They proposed one amino acid with a p$K = 8.2$ in the S_0 state and that this group has a p$K = 7.25$ in the S_2 state (*63*). A p*K* of 8.2 in the S_0 state is in good agreement with the p*K* we obtained (p$K = 8.0 \pm 0.1$) from the decrease of the S_0 EPR signal, whereas the difference is bigger between the p*K* in the S_2 state [p$K = 7.25$ (*63*) and p$K = 7.6 \pm 0.1$ (this study)]. The high p*K*s proposed (in ref *63*) are also in good agreement with the Y_Z−D1−His190 hydrogen-bonding network reported (in refs *30*, *59*, and *62*).

Another interesting amino acid candidate that could cause the decrease of the EPR signals at alkaline pH is Y_Z. Tyrosine Z is thought to be ∼8−11 Å away from the Mn cluster (*7*, *64*−*66*) and normally is not considered as a direct ligand to the Mn cluster (*2*, *7*, *64*). Oxidation of Y_Z is facilitated by deprotonation with p*K* 7.5−8 through a hydrogen bond to D1-His190 (see above), and this deprotonation could induce a magnetic interaction with the Mn cluster, causing the EPR signals to decrease. Furthermore, in calcium- or chloride-depleted or acetate-treated samples subjected to illumination, an EPR signal from the formal S_3 state can be trapped (*7*, *67*−*71*). This signal has been identified as a split signal originating from $S_2Y_Z^{\bullet}$, showing that even though Y_Z may not ligate to the Mn cluster it can definitely affect the magnetic properties of the Mn cluster (*7*, *67*−*71*). In addition to magnetic interactions, it is likely that the oxidation of Y_Z itself can modify the environment of the Mn cluster, possibly through a hydrogen-bonding network. This could lead to modified magnetic couplings between the Mn ions (*72*, *73*), altering the EPR signals from the Mn cluster. One example of such chemical interactions is found in acetate-inhibited PSII, where a S_2 state multiline signal is not detectable, although a spin-coupled signal from $S_2Y_Z^{\bullet}$ is observable in the formal S_3 state (*66*, *70*, *72*, *73*). In this system, a S_2 multiline signal becomes observable when Y_Z is oxidized but diamagnetic through interaction with NO (*74*).

We see one more possibility to explain our results at alkaline pH. It is possible that the pH changes might have altered the redox equilibrium between Y_Z and the Mn cluster (possibility iv). A pH-dependent donor-side equilibrium has been suggested previously (*17*, *75*). It has also been shown that the Tyr/Tyr$^{\bullet}$ redox-couple has a pH-dependent redox potential that decreases with 59 mV/pH unit as the pH is increased (*76*, *77*). Consequently, if the $Y_Z/Y_Z^{\bullet}$ redox-couple shows the same pH dependence, it is quite possible that the equilibrium $S_nY_Z^{\bullet} \rightleftharpoons S_{n+1}Y_Z$, which is normally shifted strongly to the right, could be shifted to the left at alkaline pH.

The potential of $Y_Z/Y_Z^{\bullet}$ and the S_1/S_2 couple are thought to be separated by about 40−60 mV (*17*, *78*). If the increased pH resulted in a decreased potential of $Y_Z/Y_Z^{\bullet}$, it is quite feasible that S_2 might oxidize Y_Z, shifting the equilibrium to form $S_1Y_Z^{\bullet}$. It is not clear how this would affect the EPR properties of the water oxidizing complex and Y_Z. However, our present results can rule out the most likely option that a free radical signal from $Y_Z^{\bullet}$ would become visible at the expense of the Mn-derived S_2-state EPR signals. Our EPR measurements of the tyrosine radical content in PSII (Figure 4A,B) reveal no change of the spectrum of $Y_D^{\bullet}$ in the pH titration experiment. Thus, if the manganese EPR signals were lost due to a lowered redox potential of $Y_Z^{\bullet}$, this does not result in a normal $S_1Y_Z^{\bullet}$ state. At present we find this mechanism unlikely as an explanation for the loss of the S_2 state EPR signal. In the S_0 state it is even more unlikely that the equilibrium between S_0Y_Z is shifted to, in this case, $S_{-1}Y_Z^{\bullet}$. This is improbable since $Y_Z^{\bullet}$ can be expected to be more oxidizing than S_0 at pH 8.5 [at physiological pH, $Y_Z^{\bullet}$ has been estimated to be ≥250 mV more oxidizing than the S_0 state (*17*)].

To conclude, there are several plausible reasons that the Mn-derived EPR signals from both S_0 and S_2 are reversibly lost upon incubation of PSII at extreme pHs. At present we rule out destruction of the Mn cluster or calcium and chloride depletion. Instead, the explanation may involve either structural changes in the Mn cluster (protonation or deprotonation of oxo bridges) or effects on ligands or amino acid side chains in the immediate vicinity of the Mn cluster. Identification of the origin of our pH-dependent effects on the S_0 and S_2 multiline EPR signals might provide vital information about central issues in the chemistry of the Mn cluster. Therefore, studies involving other spectroscopic techniques are in progress to elucidate the reversible events induced in the oxygen-evolving cluster by simple pH changes. We have also commenced studies on how pH affects the oxygen-evolving cluster in the other S states.

ACKNOWLEDGMENT

We acknowledge Sindra Peterson, Fikret Mamedov, Karin Åhrling, David Britt, Ann Magnuson, Warrick Hillier, and Gerald Babcock for useful discussions and reading of the manuscript.

REFERENCES

1. Barber, J., Nield, J., Morris, E. P., Zheleva, D., and Hankamer, B. (1997) *Physiol. Plant. 100*, 817−827.
2. Diner, B. A., and Babcock, G. T. (1996) in *Oxygenic Photosynthesis: The Light Reactions* (Ort, D. R., and Yocum, C. F., Eds.) pp 213−247, Kluwer Academic Publishers, Dordrecht, The Netherlands.
3. Renger, G. (1997) *Physiol. Plant. 100*, 828−841.
4. Britt, D. R. (1996) in *Oxygenic Photosynthesis: The Light Reactions* (Ort, D. R., and Yocum, C. F., Eds.) pp 137−164, Kluwer Academic Publishers, Dordrecht, The Netherlands.
5. Hoganson, W. C., and Babcock, G. T. (1997) *Science 277*, 1953−1956.
6. Tommos, C., and Babcock, G. T. (1998) *Acc. Chem. Res. 31*, 18−25.
7. Peloquin, J. M., Campbell, K. A., and Britt, R. D. (1998) *J. Am. Chem. Soc. 120*, 6840−6841.
8. Haumann, M., and Junge, W. (1999) *Biochim. Biophys. Acta 1411*, 86−91.
9. Debus, R. J. (2000) in *Metal Ions in Biological Systems* (Sigel, A., and Sigel, H., Eds.) pp 657−710, Marcel Dekker, New York.
10. Debus, R. J. (1992) *Biochim. Biophys. Acta 1102*, 269−352.
11. Yachandra, V. K., Sauer, K., and Klein, M. P. (1996) *Chem. Rev. 96*, 2927−2950.
12. Åhrling, K. A., Smith, P. J., and Pace, R. J. (1998) *J. Am. Chem. Soc. 120*, 13202−13214.
13. Hasegawa, K., Kusunoki, M., Inoue, Y., and Ono, T.-a. (1998) *Biochemistry 37*, 9457−9465.
14. Zheng, M., and Dismukes, G. C. (1996) *Inorg. Chem. 35*, 3307−3319.
15. Kok, B., Forbush, B., and McGloin, M. (1970) *Photochem. Photobiol. 11*, 457−475.
16. Styring, S., and Rutherford, A. W. (1987) *Biochemistry 26*, 2401−2405.
17. Vass, I., and Styring, S. (1991) *Biochemistry 30*, 830−839.
18. Dismukes, G. C., and Siderer, Y. (1981) *Proc. Natl. Acad. Sci. U.S.A. 78*, 274−278.
19. Åhrling, K. A., and Styring, S. (2000) in *Probing Photosynthesis* (Yunus, Mohanty, P., and Pathre, Eds.) Taylor and Francis, Ltd., London, U.K. (in press).
20. Åhrling, K. A., Peterson, S., and Styring, S. (1997) *Biochemistry 36*, 13148−13152.
21. Messinger, J., Robblee, J. H., Yu, W. O., Sauer, K., Yachandra, V. K., and Klein, M. P. (1997) *J. Am. Chem. Soc. 119*, 11349−11350.
22. Åhrling, K. A., Peterson, S., and Styring, S. (1998) *Biochemistry 37*, 8115−8120.
23. Conjeaud, H., and Mathis, P. (1980) *Biochim. Biophys. Acta 590*, 353−359.
24. Renger, G., and Voelker, M. (1982) *FEBS Lett. 149*, 203−207.
25. Conjeaud, H., and Mathis, P. (1986) *Biophys. J. 49*, 1215−1221.
26. Lavergne, J., and Junge, W. (1993) *Photosynth. Res. 38*, 279−296.
27. Rappaport, F., and Lavergne, J. (1997) *Biochemistry 36*, 15294−15302.
28. Diner, B. A., Force, D. A., Randall, D. W., and Britt, R. D. (1998) *Biochemistry 37*, 17931−17943.
29. Haumann, M., Mulkidjanian, A., and Junge, W. (1999) *Biochemistry 38*, 1258−1267.
30. Mamedov, F., Sayre, R. T., and Styring, S. (1998) *Biochemistry 37*, 14245−14256.
31. Vass, I., Koike, H., and Inoue, Y. (1985) *Biochim. Biophys. Acta 810*, 302−309.
32. Ono, T.-a., and Inoue, Y. (1990) *Biochim. Biophys. Acta 1015*, 373−377.
33. Cole, J., Boska, M., Blough, N. V., and Sauer, K. (1986) *Biochim. Biophys. Acta 848*, 41−47.
34. Pace, R. J., Smith, P., Bramley, R., and Stehlik, D. (1991) *Biochim. Biophys. Acta 1058*, 161−170.
35. Arnon, D. I. (1949) *Plant Physiol. 24*, 1−15.
36. Messinger, J., and Renger, G. (1994) *Biochemistry 33*, 10896−10905.
37. Geijer, P., Deák, Z., and Styring, S. (1998) in *Photsynthesis: Mechanisms and Effects* (Garab, G., Ed.) Proceedings of the XIth International Congress on Photosynthesis, pp 1283−1286, Elsevier Academic Publishers, Amsterdam.
38. Deák, Z., Peterson, S., Geijer, P., Åhrling, K. A., and Styring, S. (1999) *Biochim. Biophys. Acta 1412*, 246−249.
39. Force, D. A., Randall, D. W., Lorigan, G. A., Clemens, K. L., and Britt, R. D. (1998) *J. Am. Chem. Soc. 120*, 13321−13333.
40. Homann, P. H. (1988) *Biochim. Biophys. Acta 934*, 1−13.
41. Yocum, C. F. (1991) *Biochim. Biophys. Acta 1059*, 1−15.
42. Rutherford, A. W., Zimmermann, J.-L., and Boussac, A. (1992) in *The Photosystems: Structure, Function and Molecular Biology* (Barber, J., Ed.) pp 179−229, Elsevier Science Publishers B.V., Amsterdam.
43. Boussac, A., and Rutherford, A. W. (1994) *Biochem. Soc. Trans. 22*, 352−358.
44. Lindberg, K. (1996) Ph.D. Thesis, Gothenburg University and Chalmers University of Technology, Gothenburg, Sweden.
45. van Vliet, P. (1996) Ph.D. Thesis, Agricultural University, Wageningen, The Netherlands.
46. Campbell, K. A., Gregor, W., Pham, D. P., Peloquin, J. M., Debus, R. J., and Britt, R. D. (1998) *Biochemistry 37*, 5039−5045.
47. Baldwin, M. J., Gelasco, A., and Pecoraro, V. L. (1993) *Photosynth. Res. 38*, 303−308.
48. Baldwin, M. J., Stemmler, T. L., Riggs-Gelasco, P. J., Kirk, M. L., Penner-Hahn, J. E., and Pecoraro, V. L. (1994) *J. Am. Chem. Soc. 116*, 11349−11356.
49. Dubé, C. E., Wright, D. W., Pal, S., Bonitatebus, P. J., Jr., and Armstrong, W. H. (1998) *J. Am. Chem. Soc. 120*, 3704−3716.
50. Michaud-Soret, I., Jacquamet, L., Debaecker-Petit, N., Le Pape, L., Barynin, V. V., and Latour, J.-M. (1998) *Inorg. Chem. 37*, 3874−3876.
51. DeRose, V. J., Yachandra, V. K., McDermott, A. E., Britt, R. D., Sauer, K., and Klein, M. P. (1991) *Biochemistry 30*, 1335−1341.
52. Nixon, P. J., and Diner, B. A. (1992) *Biochemistry 31*, 942−948.
53. Tang, X.-S., Diner, B. A., Larsen, B. S., Gilchrist, M. L., Jr., Lorigan, G. A., and Britt, R. D. (1994) *Proc. Natl. Acad. Sci. U.S.A. 91*, 704−708.
54. Chu, H.-A., Nguyen, A. P., and Debus, R. J. (1995) *Biochemistry 34*, 5839−5858.

55. Magnuson, A., and Andréasson, L.-E. (1997) *Biochemistry 36*, 3254−3261.
56. Steenhuis, J. J., and Barry, B. A. (1997) *J. Phys. Chem. B. 101*, 6652−6660.
57. Hundelt, M., Hays, A.-M. A., Debus, R. J., and Junge, W. (1998) *Biochemistry 37*, 14450−14456.
58. Ghirardi, M. L., Preston, C., and Seibert, M. (1998) *Biochemistry 37*, 13567−13574.
59. Hays, A.-M. A., Vassiliev, I. R., Golbeck, J. H., and Debus, R. J. (1999) *Biochemistry 38*, 11851−11865.
60. Svensson, B., Vass, I., Cedergren, E., and Styring, S. (1990) *EMBO J. 9*, 2051−2059.
61. Svensson, B., Etchebest, C., Tuffery, P., van Kan, P. J. M., Smith, J., and Styring, S. (1996) *Biochemistry 35*, 14486−14502.
62. Hays, A.-M. A., Vassiliev, I. R., Golbeck, J. H., and Debus, R. J. (1998) *Biochemistry 37*, 11352−11365.
63. Rappaport, F., and Lavergne, J. (1991) *Biochemistry 30*, 10004−10012.
64. Boussac, A., Zimmermann, J.-L., Rutherford, A. W., and Lavergne, J. (1990) *Nature 347*, 303−306.
65. MacLachlan, D. J., Nugent, J. H. A., Warden, J. T., and Evans, M. C. W. (1994) *Biochim. Biophys. Acta 1188*, 325−334.
66. Lakshmi, K. V., Eaton, S. S., Eaton, G. R., and Brudvig, G. W. (1999) *Biochemistry 38*, 12758−12767.
67. Boussac, A., Zimmermann, J.-L., and Rutherford, A. W. (1989) *Biochemistry 28*, 8984−8989.
68. Gilchrist, M. L., Jr., Ball, J. A., Randall, D. W., and Britt, R. D. (1995) *Proc. Natl. Acad. Sci. U.S.A. 92*, 9545−9549.
69. Tang, X.-S., Randall, D. W., Force, D. A., Diner, B. A., and Britt, R. D. (1996) *J. Am. Chem. Soc. 118*, 7638−7639.
70. Force, D. A., Randall, D. W., and Britt, R. D. (1997) *Biochemistry 36*, 12062−12070.
71. MacLachlan, D. J., and Nugent, J. H. A. (1993) *Biochemistry 32*, 9772−9780.
72. Szalai, V. A., and Brudvig, G. W. (1996) *Biochemistry 35*, 1946−1953.
73. Szalai, V. A., Kühne, H., and Brudvig, G. W. (1998) *Biochemistry 37*, 13594−13603.
74. Szalai, V. A., and Brudvig, G. W. (1996) *Biochemistry 35*, 15080−15087.
75. Buser, C. A., Diner, B. A., and Brudvig, G. W. (1992) *Biochemistry 31*, 11449−11459.
76. Magnuson, A., Frapart, Y., Abrahamsson, M., Horner, O., Åkermark, B., Sun, L., Girerd, J.-J., Hammarström, L., and Styring, S. (1999) *J. Am. Chem. Soc. 121*, 89−96.
77. Tommos, C., Skalicky, J. J., Pilloud, D. L., Wand, A. J., and Dutton, P. L. (1999) *Biochemistry 38*, 9495−9507.
78. Vos, M. H. (1990) Ph.D. Thesis, State University of Leiden, Leiden, The Netherlands.

BI992878C